Enhancing Anomaly Detection in Pedestrian Walkways using Improved Sparrow Search Algorithm with Parallel Features Fusion Model

Y. Sreeraman[1], D. Jagadeesan[1,*], J. Jegan[1], T. Vivekanandan[1], A. Srinivasan[2], G. Asha[3]

[1]Department of Computer Science and Engineering, School of Technology, The Apollo University, Chittoor, Andhra Pradesh, India;
[2]Department of Computer Science and Engineering (Data Science), Sreenivasa Institute of Technology and Management Studies, Chittoor, Andhra Pradesh, India;
[3]Department of Electronics and Communication Engineering, Adhiparasakthi College of Engineering, Kalavai, Ranipet District, Tamil Nadu, India;
Emails: sramany@gmail.com; djagadeesanphd@gmail.com; jegan.deepa@gmail.com; stvanand@gmail.com; srini.vit@gmail.com; ashajagadeesan@gmail.com
[*]Corresponding Author: djagadeesanphd@gmail.com

Abstract

Anomaly detection in pedestrian walkways is a vital research area, widely employed to enhance the safety of the pedestrians. Because of the widespread usage of the video surveillance systems and the increasing number of captured videos, the conventional manual examination of labeling abnormal events is a laborious process. Therefore, an automatic surveillance system to accurately detect anomalies becomes essential among computer vision researchers. Presently, the development of deep learning (DL) models has gained significant interest in different computer vision processes namely object classification and object detection, and these applications were depending on supervised learning that required labels. This article develops an Improved Meta-heuristic with Parallel Features Fusion Model for Anomaly Detection in Pedestrian Walkways (IMPFF-ADPW) method. The main aim of the IMPFF-ADPW approach is to recognize the existence of anomalies in pedestrian walkways. To obtain this, the IMPFF-ADPW method applies a joint bilateral filter (JBF) for the process of noise removal. Besides, a parallel fusion process comprising NasNet Mobile and Darknet-53 models can be utilized for feature extraction. For the anomaly detection method, the deep autoencoder (DAE) model is applied and its hyperparameters are finetuned by using an improved sparrow search algorithm (ISSA). A wide of experimental outcomes can be applied to the UCSD database to illustrate the betterment of the IMPFF-ADPW methodology. The simulation values indicated the enhanced performance of the IMPFF-ADPW method over other existing techniques.

Keywords: Computer vision; Pedestrian walkways; Anomaly detection; Metaheuristics; Deep learning

1. Introduction

Transportation system becomes an underlying basis for the economic development of all other countries [1]. Nonetheless, many cities in various parts of the world are now facing an uncontrollable development in traffic volume, causing significant challenges, like degradation of the quality of life in the modern world, traffic jams, delays, emergencies, accidents, high fuel prices, and increase of CO2 emission [2]. In most cases, the anomaly prediction approach applies unsupervised and semi-supervised learning algorithms. The primary objective is to find the anomaly forecast scheme used in road traffic incidents and focuses on appliances such as trespassers, atmosphere, communication, and vehicles [3]. It also observed that the scope of this has to enclose the class of abnormalities, the ability of the system in application contents, the nature of the input dataset and the representation, probability of supervised learning, anomaly prediction outcomes, and terminating conditions [4]. Anomalies were predicted using a recently established scheme as soon as the general patterns were defined [5].

Doi: https://doi.org/10.54216/FPA.140210
Received: July 17, 2023 Revised: November 09, 2023 Accepted: January 08, 2024

Lately, different approaches have been used for predicting pedestrian walking that fits the bounding box for the pedestrian accessible from the image [6]. It has gradually attracted the attention of several research workers in the computer vision (CV) field and is a substantial component for different human-based fields including driverless cars, person inspection, automated traffic signalling, etc [7]. However, the predefined model was not fit for solving the difficulty of the model termed scaling problem which keeps the same reason for the outcomes of the pedestrian recognition technique. The conventional techniques have been maintained to resolve the scaling problems on 2-D size [8]. Initially, brute-force data was enhanced to increase the ability of the scale-invariance mechanism. Following, individual approaches with different scale filters were applied in all the instances with different sizes. Then, the incidence of intra-class variance of tiny and maximum instances makes it difficult to conquer the considerably different attribute responses together with a single method [9]. To exploit considerably different features with different scales, the divide-and-conquer model was exploited for solving scale variance problems. Finally, the study deployed Deep Learning (DL) based on the anomaly prediction technique [10]. Firstly, Convolution Neural Network (CNN) can be exploited and classified as the existence of objects.

This study develops an Improved Metaheuristics with Parallel Features Fusion Model for Anomaly Detection in Pedestrian Walkways (IMPFF-ADPW) technique. The IMPFF-ADPW method applies a joint bilateral filter (JBF) for the noise removal process. Besides, a parallel fusion process comprising NasNet Mobile and Darknet-53 models is utilized for feature extraction. For the anomaly detection system, the deep autoencoder (DAE) model is applied and its hyperparameters are finetuned by using an improved sparrow search algorithm (ISSA). A widespread of experimental values can be performed on the UCSD database to validate the betterment of the IMPFF-ADPW approach.

2. Related Works

Alohali et al. [11] examine an Anomaly Detection (AD) in Pedestrian Walkways for ITSs utilizing Federated Learning and HHO (ADPW-FLHHO) approach on RSIs. The projected ADPW-FLHHO system concentrations on the classification and detection of ADs, using vehicles from the pedestrian walkway. To achieve this, the study utilizes the HybridNet approach for the generation of feature vectors. Besides, the HHO system can be executed for the optimum hyper-parameter tuned method. Murugan et al. [12] presented a Region-based Scalable CNN (RS-CNN). The presented approach utilized a region-based proposal for fast detection and properly enforced scalability problems. The RS-CNN approach can be validated by employing various video orders in the UCSD-AD database.

In [13], the authors challenge the problem in DL structure by assuming motion data of the entire pedestrian and its communication with the crowd. Especially, inspired by the residual learning in DL, the authors present to forecast displacement among neighboring frames to all the pedestrians in order. For predicting such displacement, the author's strategy is a crowd interaction DNN (CIDNN), which adopts the several importance of distinct pedestrians for displacement estimate of target pedestrian. Boyuan and Muqing [14] present a pedestrian detection method dependent upon an enhanced YOLO-v4 approach that regards either recognition accuracy or effectiveness. The detection method integrates a novel kind of SPP (Spatial Pyramid Pooling) and K-means clustering approach with YOLO-v4 algorithm for simpler extracting features.

The authors in [15], employ the Spectral Edge image fusion approach for fusing visible RGB and IR images, an earlier method employing an NN-based pedestrian recognition method. The procedure of image fusion allows the typical RGB object recognition network with no need the structural changes, which can be essential for handling multi-spectral input. Hara et al. [16] examine the approach for estimating the low of pedestrian walking on the footways. The aim is to obtain maximum accuracy with extensive region coverage at a minimum price. In pedestrian recognition, faces and backs of heads can be individually identified to understand the moving direction of pedestrians and their presence by executing CNN and LSTM.

In [17], the authors detect that it is much greater effective for learning and predicting pedestrian paths in 3D space as the human gesture and its performance designs are optimistically represented in 3D space. Accordingly, the authors utilize a stereo camera system for detecting and tracking human pose with DNNs. In the pose estimate, these twin DNNs fulfill the stereo consistency restriction. Jeong et al. [18] utilize DL approaches to overcome the restrictions of the present smartphone-based PDR algorithm. A CNN approach was utilized for classifying the smartphone positions; afterward, suitable sensor data can be chosen and modified. The LSTM approach was utilized for estimating the user step length.

3. The Proposed Model

In this article, a new IMPFF-ADPW model is established for detecting anomalies. The major intention of the IMPFF-ADPW approach is to recognize the existence of anomalies in the pedestrian walkways. To obtain this,

Doi: https://doi.org/10.54216/FPA.140210
Received: July 17, 2023 Revised: November 09, 2023 Accepted: January 08, 2024

the IMPFF-ADPW algorithm comprises JBF-based pre-processing, parallel fusion process, DAE classification, and ISSA-based hyperparameter tuning. Fig. 1 signifies the working flow of the IMPFF-ADPW system.

A. Image Pre-processing

The JBF method is applied to remove the presence of noise. The typical JBF filter highly maintains the edge details dependent upon the image intensities [19]. JBF helps to preserve edge information existing in the images. However, with lower intensity, which filter can be incapable of maintaining the edge details of the images. Hence, the presented effort employs the JBF approach to address these drawbacks. The initial principal element was applied as the guidance image exchanging the kernel filter range for efficiently preserving the edge data over the typical filter. The expression of the JBF filtering method is represented by:

$$I_{BF}(j,k,b) = \frac{1}{i(j,k)} \sum \{ G_{\sigma_d}(j-p, k-q) \quad (1)$$

$$* \, c_{\sigma_r}[I_{Pc}(j,k) - I_{Pc}(p,q)] I(p,q,b)\}$$

In Eq. (1), I_{Pc} shows the input images at pixel location (j,k), represents the first principal component, b refers to the index of spectral band σ_d and σ_r denotes the domain and range parameters, and p and q indicate the pixel point of the image. The normalization factor of JBF can be described by using Eq. (2):

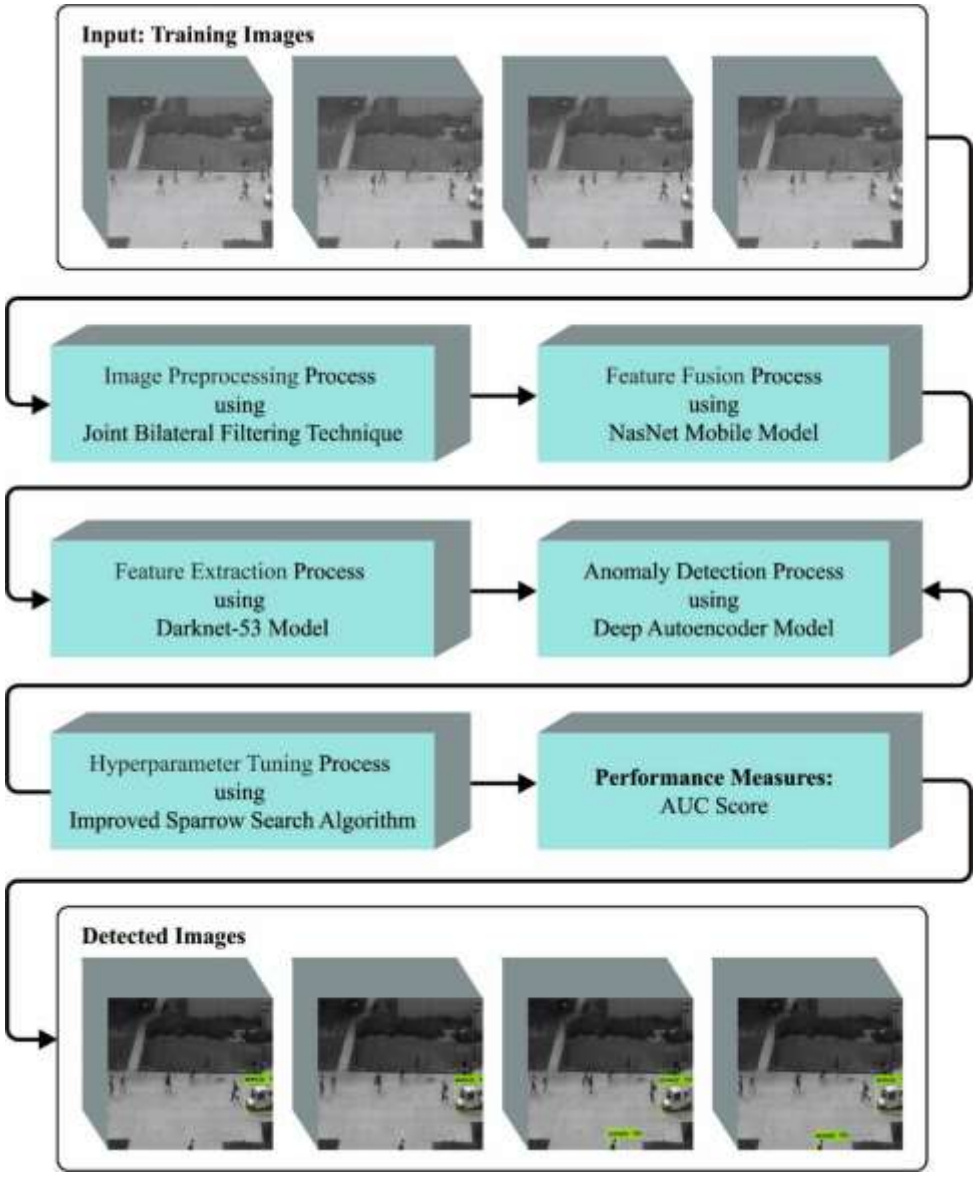

Figure 1: Overall flow of IMPFF-ADPW approach

Doi: https://doi.org/10.54216/FPA.140210
Received: July 17, 2023 Revised: November 09, 2023 Accepted: January 08, 2024

$$i(j,k) = \sum \{ G_{\sigma_d}(j-p, k-q) \quad (2)$$

$$* c_{\sigma_r}\left(I_{Pc}(j,k) - I_{Pc}(p.q)\right)\}$$

The σ_r parameter is called an edge-preserving factor and a large value creates Gaussian blurring, thus it can be desired that smaller. The edge information was preserved and the image quality was improved by using these filters for preprocessing. Thus, the outcomes from these phases assist in better feature extraction.

B. Parallel Feature Fusion Model

At this stage, the parallel feature fusion process is performed. In this work, NASNet Mobile and Darknet-53 are utilized as two pre-trained models for extracting deep features [20]. NASNet comprises two major functions, reduction cell, and normal cell NASNet implements the operation on smaller datasets and later transfers the block to large datasets for getting a mean average precision (mAP). The model learns an effective feature for detecting images and its size is 224x224 pixels. The convolution cell is used to decrease the processing costs and improve the classifier performance. Normal cells and reduction cells are established with this convolution cell to expand the usage of NASNet for images of any size.

Darknet53 is a 53-layered CNN. Here, the feature extractor includes the sequence of convolution layers at 1x1 and 3x3 dimensions. A Leaky rectified linear activation unit (LeakyReLU) layer and a batch normalization (25) layer followed all the convolutional layers. After the convolutional layer, it can prevent overfitting and accelerate network convergence. The LeakyReLU with leakage correction raises the nonlinearity of the network architecture. The transfer learning method was used for extracting DL features and training fine-tuned models. Remove the FC layer and add a new layer for the NasNet Mobile.

A Parallel Priority (PP) called parallel features fusion approach was introduced in this study. The inspiration behind this is to decrease the feature vectors with increasingly relevant features. The technique was dependent upon the three crucial phases. Initially, based on the entropy value, padding makes the equivalent size of these two vectors. Next, the entropy values are calculated from the huge feature size vector and used for the padding of small feature vectors and it can be mathematically computed as follows:

$$h_a(\lambda) = \frac{1}{1-a} \log\left(\sum_{i=1}^{h} P_i^a\right) \quad (3)$$

In Eq. (3), λ indicates the feature point of the high dimensional feature vector, P_i^a shows the probability of all the feature points, and n refers to the overall amount of features. Padding is performed based on the h for small size feature vector using Eq. (4):

$$padding = (FV, h) \leftarrow \widetilde{FV} \quad (4)$$

In Eq. (4), FV and $\widetilde{FV}$ refer to the small and large-size feature vectors. After padding, the feature vector attained can be represented as $\widetilde{FV}$. Next, based on higher feature values, the priority of feature values was defined.

$$vector = priority\left(\widetilde{FV}, \widetilde{FV}\right) \quad (5)$$

In Eq. (5), the function priority first chooses the high values for i^{th} and j^{th} features. Next, the mean value will be calculated for the whole vector, and determine threshold function for the last fusion given below:

$$Th = \begin{cases} Fus(k) & \text{for vector } (i) \geq \mu \\ Ignore, & \text{Elsewhere} \end{cases} \quad (6)$$

In Eq. (6), $Fus(k)$ denotes the final fused vector of dimension $N \times 1290$.

C. Anomaly Detection Using Optimal DAE Model

The DAE approach is used for the anomaly detection process. Autoencoder (AE) is a 3-layer unsupervised NN model [21]. It is the simple process of NN that is utilized for learning representation namely size reduction or feature selection and recreating the input pattern in the output layers. The dimensions of the input and output layers are similar to the symmetrical structure. Compared to the visible layer, the hidden state from the network model generally has fewer neurons. By employing a limited amount of neurons, an effort was developed to represent or encode the input in a more compressed manner, which captures the relevant features of the input vector. According to the MSE loss function, the training of AE is performed by using a BP model as in FFNN. The training model comprises two phases, coding, and decoding. By exploiting the weight condition of the lower half layer the input

Doi: https://doi.org/10.54216/FPA.140210
Received: July 17, 2023 Revised: November 09, 2023 Accepted: January 08, 2024

was encoded during the coding stage in a hidden description. Utilizing the conditions of the upper half layer stage, a similar input is tried to reconstruct in the representation of coding during the decoding process. Assume X as data with m features and n samples. y refers to the encoder output (viz., decreased representation of X). The equations of encoded and decoded functions for AE are shown below.

$$Y = f(wX + b) \tag{7}$$

$$\acute{X} = g(\acute{w}Y + b) \tag{8}$$

Where w and b refer to the adjustable parameter, f, and g are the activation function, $\acute{w}$ shows the weighted $(\acute{X})$ transpose, and $\acute{X}$ indicates the recreated input vectors in the resulting layer. Fig. 2 portrays the framework of DAE.

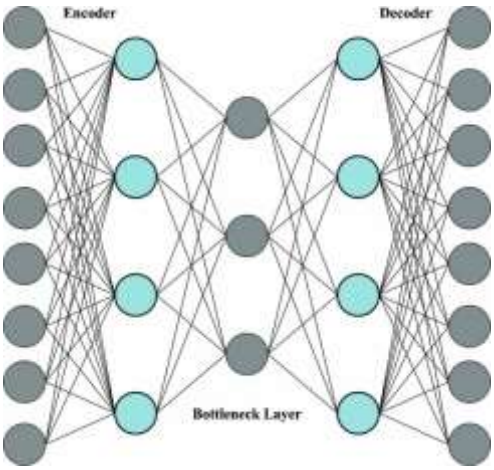

Figure 1: Architecture of DAE

Training an AE includes finding parameters w and b that reduce the errors amongst $\acute{X}$ the reconstruction data and X the input data.

Finally, the ISSA selects the hyperparameter values of the DAE algorithm. SSA is a population optimization method that completes the food acquisition by continuously updating the location of the discoverers, followers, and vigilant while foraging, and the position of the optimum food is the optimum solution obtained so far [22].

$$X = [x_1, x_2, \dots, x_n] \tag{9}$$

$$F = [f(x_1), f(x_2), \dots, f(x_n)] \tag{10}$$

The position updating equation of the discoverer can be given as follows:

$$x_{ij}^{t+1} = \begin{cases} x_{ij}^{t} \cdot \exp\left(\dfrac{-i}{\alpha \times iter_{\max}}\right) & R_2 < ST \\ x_{ij}^{t} + Q \cdot L & R_2 \geq ST \end{cases} \tag{11}$$

Where t characterizes the existing iteration count, x_{ij}^{t} signifies the location of i^{th} sparrows in the j^{th} dimensions at t^{th} generation, and $\alpha \in (0,1)$, $iter_{\max}$ shows the maximal iteration count, R_2 represents the alarm value, ST is the safety threshold, L represents the identity matrix of $1 \times dim$, Q refers to the arbitrary integer that follows the uniform distribution, and the dimension is dim.

The position updating of the follower is shown below:

$$x_{ij}^{t+1} = \begin{cases} Q \cdot \exp\left(\dfrac{x_{worst}^{t} - x_{ij}^{t}}{i^2}\right) & i \in (n/2, +\infty) \\ x_{p}^{t+1} + \left|x_{ij}^{t} - x_{p}^{t+1}\right| \cdot Z^{+} \cdot L & i \in [0, n/2] \end{cases} \tag{12}$$

In Eq. (12), x_{worst}^{t} signifies the individual location with worst adaptation of t, x_{p}^{t+1} denotes the individual location with better adaptation in $f + 1$, Z indicates a matrix of $1 \times dim$, and all the components from the matrix are arbitrarily fixed to -1 or 1, $Z^{+} = Z^{T}(ZZ^{T})^{-1}$. If $i > nl2$, it implies that the i^{th} entrants have not required food and are in hungry extreme form. The position updating of the vigilante is shown below:

Doi: https://doi.org/10.54216/FPA.140210
Received: July 17, 2023 Revised: November 09, 2023 Accepted: January 08, 2024

$$x_{ij}^{t+1} = \begin{cases} x_{best}^{t} + \beta \cdot \left| x_{ij}^{t} - x_{best}^{t} \right| & f_i \neq f_g \\ X_{best}^{t} + k \cdot \left(\dfrac{x_{ij}^{t} - x_{best}^{t}}{|f_i - f_w| + \varepsilon} \right) & f_i = f_g \end{cases} \quad (13)$$

In Eq. (13), x_{best}^{t} shows the position of the global optimum at t generation, the control step is, $k \in [-1,1]$, follows the uniform distribution range of [0,1], the fitness values of the present global worse and fittest individuals is f_g and f_w, ε is constant, f_i indicates the fitness value of existing individuals.

The classical SSA is proposed to overcome the challenges of SSA easily stuck into local optima. Population elite strategy and Tent chaos mapping are used for initializing the multiplicity of the sparrow population and to increase the initial solution quality:

$$x_{m+1} = f(x_m) = \begin{cases} x_m/\beta & x_m \in [0, \beta) \\ (1 - x_m)/(1 - \beta) & x_m \in [\beta, 1] \end{cases} \quad (14)$$

When $\beta = \frac{1}{2}$, then the system is in a short cycle state, thus the value is commonly not taken. The initial value x_m of the system and the system parameter β need to be different to avoid conversion to the cyclical system.

The reverse learning model is used to replace the sparrow locality. The dynamic edge of the elite sparrow can be attained while choosing the elite sparrow based on the fitness value of the upgraded sparrow, and the reverse anti-sparrow population can be attained to resolve the best solution, and the newest population can be created in the sparrow, and the best sparrow was chosen as newest generation individual to resolve the problems of local optima. The assumption that the extreme point corresponds to normal individuals from the population is elite individuals,

$$Y_{m,n}^{e} = \left(Y_{m,1}^{e}, Y_{m,2}^{e}, \dots, Y_{m,D}^{e} \right) \quad (15)$$

Its reverse solution is

$$\overline{Y_{m,n}^{e}} = \left(\overline{Y_{m,1}^{e}}, \overline{Y_{m,2}^{e}}, \dots, \overline{Y_{m,D}^{e}} \right) \quad (16)$$

The elite reverse solution was given as

$$\overline{Y_{m,n}^{e}} = K(\alpha_n + \beta_n) - Y_{m,n}^{e} \quad (17)$$

In Eq. (17), K indicates the stochastic figure within [0,1] and α_n, β_n signifies the dynamic boundary, and $Y_{m,n}^{e} \in [\alpha_n, \beta_n]$.

Fitness selection is a primary aspect of the ISSA model. An encoded solution can be exploited to estimate the best candidate outcome. The accuracy value is the key condition exploited to design an FF.

$$Fitness = \max(P) \quad (18)$$

$$P = \frac{TP}{TP + FP} \quad (19)$$

Here, FP signifies false positive value and TP represents true positive value.

4. Results and Discussion

The detection performance of the IMPFF-ADPW approach is tested on three datasets, as given in Table 1. Fig. 3 demonstrates the sample images. Fig. 4 represents the anomaly-detected images.

Table 1: Description of three datasets

Dataset	UCSDPed1 (Bikers, small carts, walking across walkways)	UCSDPed2 (Bikers, small carts, walking across walkways)	Avenue (Run, throw, new object)
No. of Videos	70	28	37
Training Set	34	16	16
Testing Set	36	12	21
Dataset Length	5 min	5 min	5 min

Doi: https://doi.org/10.54216/FPA.140210
Received: July 17, 2023 Revised: November 09, 2023 Accepted: January 08, 2024

Figure 3: Sample Images

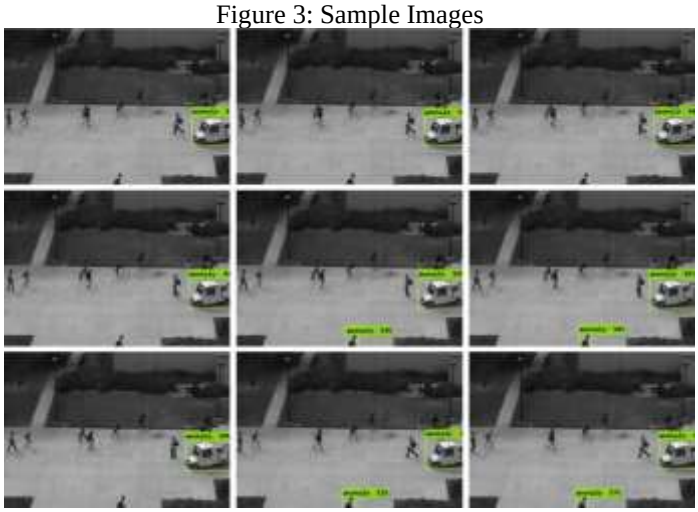

Figure 4: Anomaly Detected Images

Figure 5: $Accu_y$ curve of IMPFF-ADPW approach on UCSDPed1 database

The training accuracy TR_accu_y and VL_accu_y of the IMPFF-ADPW algorithm on the UCSDPed1 database is shown in Fig. 5. The TL_accu_y is computed by assessing the IMPFF-ADPW method under the TR dataset while the VL_accu_y is described by estimating the result on testing database. The outcome exhibits that TR_accu_y and VL_accu_y increased with increasing epoch count. Thus, the outcome of the IMPFF-ADPW technique attains a maximum in TR and TS data with maximum epoch count.

Doi: https://doi.org/10.54216/FPA.140210
Received: July 17, 2023 Revised: November 09, 2023 Accepted: January 08, 2024

Fig.6 shows the TR_loss and VR_loss investigation of the IMPFF-ADPW system on the UCSDPed1 database. The TR_loss represents the error among the original and prediction performance values on the TR dataset. The VR_loss signifies the performance metric of the IMPFF-ADPW method on the validation dataset. The accomplished finding denotes that TR_loss and VR_loss tend to reduce with maximum epoch count. It represented the high performance of the IMPFF-ADPW system and its proficiency in producing a precise classification. The minimal value of TR_loss and VR_loss reveals the maximum results of the IMPFF-ADPW system on capturing patterns and correlations.

Figure 6: Loss curve of IMPFF-ADPW approach on UCSDPed1 database

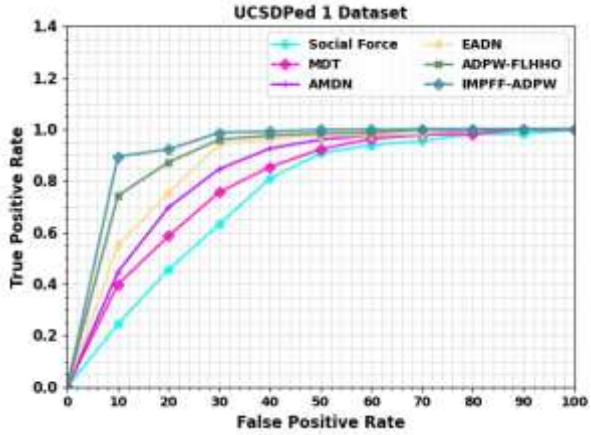

Figure 7: Detection outcome of IMPFF-ADPW system on UCSDPed1 database

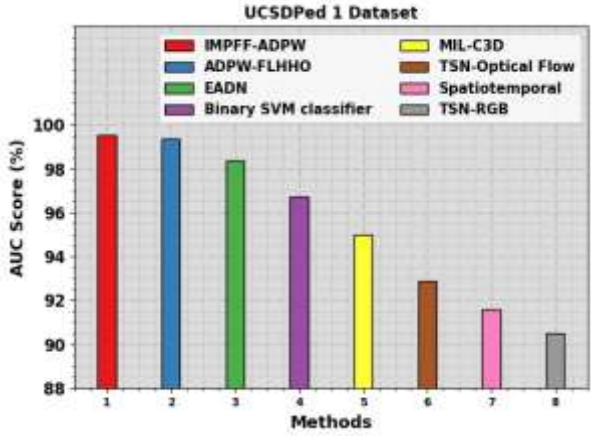

Figure 8: AUC_{score} outcome of IMPFF-ADPW method on UCSDPed1 dataset

Fig. 7 shows the detection outcomes of the IMPFF-ADPW algorithm with other approaches on the UCSDPed1 dataset. The result shows that the SF, MDT, and AMDN methods have obtained poor performance. Along with

Doi: https://doi.org/10.54216/FPA.140210
Received: July 17, 2023 Revised: November 09, 2023 Accepted: January 08, 2024

that, the EADN model has managed to report slightly enhanced results. Meanwhile, the ADPW-FLHHO algorithm has resulted in considerable performance. However, the IMPFF-ADPW technique revealed better performance.

In Fig. 8, the comparison analysis of the IMPFF-ADPW method with existing approaches with respect to the AUC score on the UCSDPed1 dataset [11]. The outcomes show that the IMPFF-ADPW approach obtains a higher AUC score of 99.53%. On the other hand, the ADPW-FLHHO, EADN, binary SVM, MIL-C3D, TSN-Optical Flow, Spatiotemporal, and TSN-RGB approaches have obtained lower AUC score values of 99.36%, 98.36%, 96.73%, 94.99%, 92.86%, 91.57%, and 90.49% correspondingly.

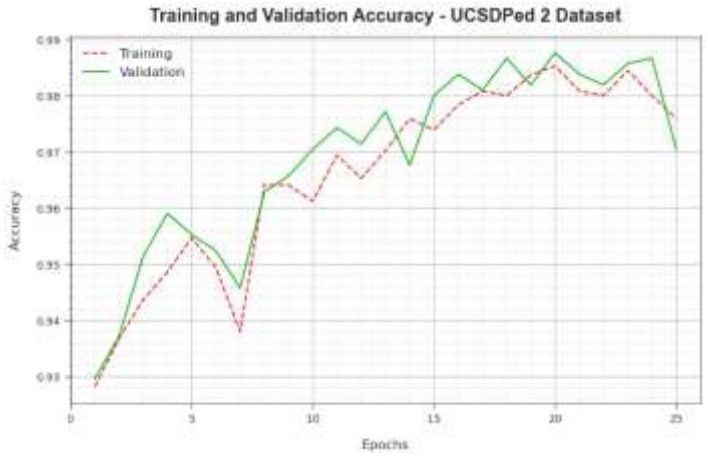

Figure 9: $Accu_y$ curve of IMPFF-ADPW approach on UCSDPed2 database

Fig. 9 shows the training accuracy TR_accu_y and VL_accu_y of the IMPFF-ADPW approach on the UCSDPed2 database. The TL_accu_y is represented by the computation of the IMPFF-ADPW system on the TR dataset while the VL_accu_y is evaluated by measuring the solution on the testing dataset. The outcome exhibits that TR_accu_y and VL_accu_y are increased with increasing epoch count. Accordingly, the solution of the IMPFF-ADPW technique gains enhancement on the TR and TS dataset with increasing epoch count.

Fig. 10 shows the TR_loss and VR_loss curves of the IMPFF-ADPW system on the UCSDPed2 database. The TR_loss describes the error amongst the original and predictive performance values on the TR dataset. The VR_loss denotes the performance measure of the IMPFF-ADPW system on the validation dataset. The outcome denotes that the TR_loss and VR_loss tend to be reduced with maximum epoch count. It characterized the greater solution of the IMPFF-ADPW system and its proficiency in producing an accurate classification. The minimized value of TR_loss and VR_loss establishes the better outcomes of the IMPFF-ADPW system in capturing patterns and relationships.

Figure 10: Loss curve of IMPFF-ADPW method on UCSDPed2 database

Doi: https://doi.org/10.54216/FPA.140210
Received: July 17, 2023 Revised: November 09, 2023 Accepted: January 08, 2024

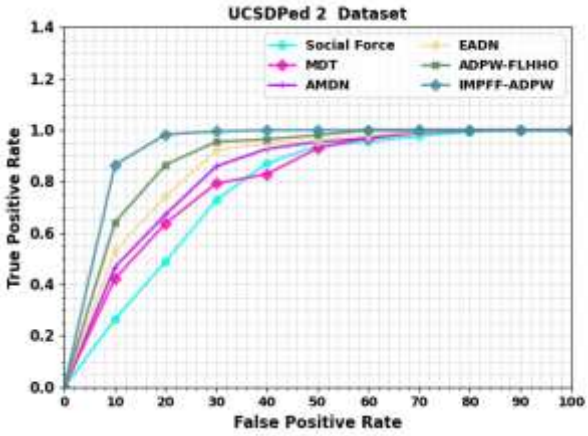

Figure 11: Detection outcome of IMPFF-ADPW method on UCSDPed2 database

Fig. 11 displays the detection outcome of the IMPFF-ADPW system with existing algorithms on the UCSDPed2 database. The outcomes show that the SF, MDT, and AMDN approaches have gained worse performance. Also, the EADN approach has managed to report slightly enhanced results. In the meantime, the ADPW-FLHHO system has resulted in considerable performance. However, the IMPFF-ADPW technique revealed better performance.

In Fig. 12, the comparison outcomes of the IMPFF-ADPW technique with other algorithms with respect to the AUC score on the UCSDPed2 dataset. The outcomes showed that the IMPFF-ADPW method obtained a superior AUC score of 99.32%. Afterwards, the ADPW-FLHHO, EADN, binary SVM, MIL-C3D, TSN-Optical Flow, Spatiotemporal, and TSN-RGB methods have attained lesser AUC score values of 99.19%, 98.30%, 97.16%, 95.50%, 94.36%, 92.48%, and 90.44% correspondingly.

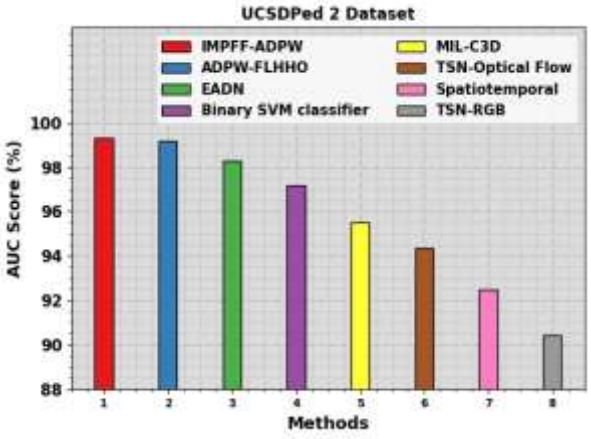

Figure 12: AUC_{score} outcome of IMPFF-ADPW algorithm on UCSDPed2 database

Figure 13: $Accu_y$ curve of IMPFF-ADPW system on Avenue database

Doi: https://doi.org/10.54216/FPA.140210
Received: July 17, 2023 Revised: November 09, 2023 Accepted: January 08, 2024

Fig. 13 displays the training accuracy TR_accu_y and VL_accu_y of the IMPFF-ADPW approach on the Avenue database. The TL_accu_y is determined by estimating the IMPFF-ADPW system on the TR dataset while the VL_accu_y is evaluated by measuring the solution on the testing dataset. The outcome exhibits that TR_accu_y and VL_accu_y increased with the maximum epoch. Thus, the outcome of the IMPFF-ADPW method attains enhancements on the TR and TS datasets with maximum epoch count.

Fig. 14 shows the TR_loss and VR_loss outcome of the IMPFF-ADPW system on the Avenue dataset. The TR_loss depicts the error amongst the prediction outcome and original values on the TR dataset. The VR_loss shows the performance metric of the IMPFF-ADPW method on the validation dataset. The outcome indicates that the TR_loss and VR_loss tend to be minimized with increased epoch count. It demonstrated the greater outcome of the IMPFF-ADPW system and its proficiency for generating accurate classification. The minimized values of TR_loss and VR_loss reveal the enhanced outcome of the IMPFF-ADPW algorithm in capturing relationships and patterns.

Figure 14: Loss curve of IMPFF-ADPW method on Avenue database

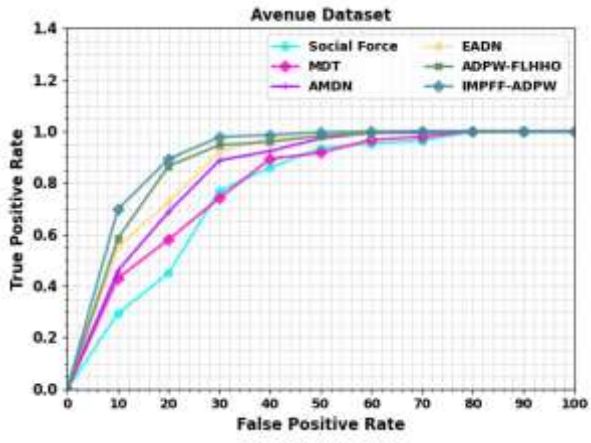

Figure 15: Detection outcome of IMPFF-ADPW system on Avenue database

Fig. 15 displays the detection results of the IMPFF-ADPW algorithm with other methods on the Avenue database. The outcomes demonstrated that the SF, MDT, and AMDN systems obtained the least result. Likewise, the EADN algorithm has managed to report slightly enhanced results. But, the ADPW-FLHHO approach has resulted in considerable performance. However, the IMPFF-ADPW approach revealed the best solution.

In Fig. 16, the comparison outcomes of the IMPFF-ADPW methodology with existing techniques concerning the AUC score on the Avenue database. The outcomes referred to the IMPFF-ADPW methodology attain a superior AUC score of 99.13%. Also, the ADPW-FLHHO, EADN, binary SVM, MIL-C3D, TSN-Optical Flow, Spatiotemporal, and TSN-RGB approaches have acquired lesser AUC score values of 98.90%, 97.78%, 96.21%, 95.02%, 93.31%, 91.41%, and 89.47% correspondingly.

Doi: https://doi.org/10.54216/FPA.140210
Received: July 17, 2023 Revised: November 09, 2023 Accepted: January 08, 2024

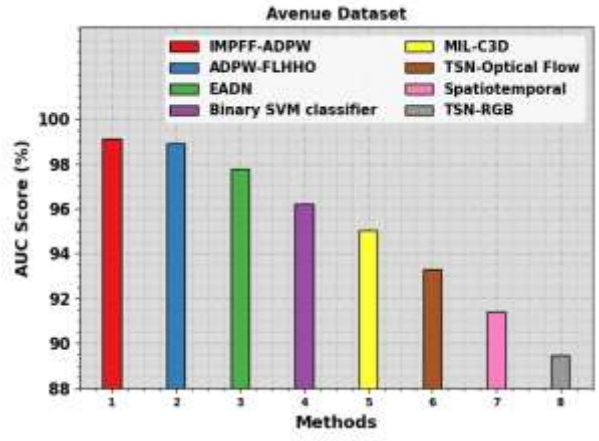

Figure 16: AUC_{score} outcome of IMPFF-ADPW algorithm on Avenue dataset

These outcomes demonstrated the greater performance of the IMPFF-ADPW method in the anomaly detection method.

5. Conclusion

In this article, a novel IMPFF-ADPW algorithm was established for detecting the anomalies. The primary objective of the IMPFF-ADPW technique is to recognize the existence of anomalies that exist in the pedestrian walkways. To obtain this, the IMPFF-ADPW approach comprises JBF-based pre-processing, parallel fusion process, DAE classification, and ISSA-based hyperparameter tuning. In this study, the hyperparameters of the DAE can be adjusted by using ISSA which helps in attaining improved detection rate. A widespread of experimental outcomes can be performed on the UCSD database to demonstrate the improved performance of the IMPFF-ADPW system. The simulation values stated the superior outcome of the IMPFF-ADPW system over other existing techniques. In the future, the ensemble voting classifier was designed to enhance the recognition rate of the IMPFF-ADPW method.

Funding: "This research received no external funding"

Conflicts of Interest: "The authors declare no conflict of interest."

References

[1] Pustokhina, I.V., Pustokhin, D.A., Vaiyapuri, T., Gupta, D., Kumar, S. and Shankar, K., 2021. An automated deep learning based anomaly detection in pedestrian walkways for vulnerable road users safety. Safety science, 142, p.105356.

[2] Dey, A., Mohammad, F., Ahmed, S., Sharif, R. and Saif, A.S., 2019. Anomaly detection in crowded scene by pedestrians behaviour extraction using long short term method: a comprehensive study. International Journal of Education and Management Engineering, 9(1), p.51.

[3] Yadav, D., Jain, A., Asati, S. and Yadav, A.K., 2023. Video Anomaly Detection for Pedestrian Surveillance. In Computer Vision and Machine Intelligence: Proceedings of CVMI 2022 (pp. 489-500). Singapore: Springer Nature Singapore.

[4] Zhang, Y., Bolten, N., Mehta, S. and Caspi, A., 2023. APE: An Open and Shared Annotated Dataset for Learning Urban Pedestrian Path Networks. arXiv preprint arXiv:2303.02323.

[5] Schaefer, M., Salari, H.E., Köckler, H. and Thinh, N.X., 2021. Assessing local heat stress and air quality with the use of remote sensing and pedestrian perception in urban microclimate simulations. Science of the total environment, 794, p.148709.

[6] Ertz, O., Fischer, A., Ghorbel, H., Hüsser, O., Sandoz, R. and Scius-Bertrand, A., 2021. Citizen Participation & Digital Tools to Improve Pedestrian Mobility in Cities. The International Archives of the Photogrammetry, Remote Sensing and Spatial Information Sciences, 46, pp.29-34.

[7] Pan, H., Luo, Y., Zeng, L., Shi, Y., Hang, J., Zhang, X., Hua, J., Zhao, B., Gu, Z. and Buccolieri, R., 2023. Outdoor Thermal Environment Regulation of Urban Green and Blue Infrastructure on Various Types of Pedestrian Walkways. Atmosphere, 14(6), p.1037.

[8] Dewi, D.I.K., Rakhmatulloh, A.R. and Syahri, E.K., 2022. Adaptation of the pedestrian walkways design along the Trans Semarang Bus Corridor to COVID-19. International journal of built environment and sustainability, 9(2-3), pp.25-37.

Doi: https://doi.org/10.54216/FPA.140210
Received: July 17, 2023 Revised: November 09, 2023 Accepted: January 08, 2024

[9] Lui, A.K.F., Chan, Y.H. and Leung, M.F., 2022, April. Modelling of pedestrian movements near an amenity in walkways of public buildings. In 2022 8th International Conference on Control, Automation and Robotics (ICCAR) (pp. 394-400). IEEE.
[10] Perera, I.M.H., Athapaththu, C.J. and Mampearachchi, W.K., 2020. Design of a porous concrete mixture for drainage coverslab in pedestrian walkways. Transportation Research Procedia, 48, pp.3678-3695.
[11] Alohali, M.A., Aljebreen, M., Nemri, N., Allafi, R., Duhayyim, M.A., Ibrahim Alsaid, M., Alneil, A.A. and Osman, A.E., 2023. Anomaly Detection in Pedestrian Walkways for Intelligent Transportation System Using Federated Learning and Harris Hawks Optimizer on Remote Sensing Images. Remote Sensing, 15(12), p.3092.
[12] Murugan, B.S., Elhoseny, M., Shankar, K. and Uthayakumar, J., 2019. Region-based scalable smart system for anomaly detection in pedestrian walkways. Computers & Electrical Engineering, 75, pp.146-160.
[13] Xu, Y., Piao, Z. and Gao, S., 2018. Encoding crowd interaction with deep neural network for pedestrian trajectory prediction. In Proceedings of the IEEE conference on computer vision and pattern recognition (pp. 5275-5284).
[14] Boyuan, W. and Muqing, W., 2020, December. Study on pedestrian detection based on an improved YOLOv4 algorithm. In 2020 IEEE 6th International Conference on Computer and Communications (ICCC) (pp. 1198-1202). IEEE.
[15] French, G., Finlayson, G. and Mackiewicz, M., 2018. Multi-spectral pedestrian detection via image fusion and deep neural networks. Journal of Imaging Science and Technology, pp.176-181.
[16] Hara, Y., Uchiyama, A., Umedu, T. and Higashino, T., 2018, October. Sidewalk-level people flow estimation using dashboard cameras based on deep learning. In 2018 eleventh international conference on mobile computing and ubiquitous network (ICMU) (pp. 1-6). IEEE.
[17] Zhong, J., Sun, H., Cao, W. and He, Z., 2020. Pedestrian motion trajectory prediction with stereo-based 3D deep pose estimation and trajectory learning. IEEE access, 8, pp.23480-23486.
[18] Jeong, S., Min, J. and Park, Y., 2021. Indoor positioning using deep-learning-based pedestrian dead reckoning and optical camera communication. IEEE access, 9, pp.133725-133734.
[19] Alamgir, F.M. and Alam, M.S., 2023. An artificial intelligence driven facial emotion recognition system using hybrid deep belief rain optimization. Multimedia Tools and Applications, 82(2), pp.2437-2464.
[20] Rehman, S., Khan, M.A., Alhaisoni, M., Armghan, A., Tariq, U., Alenezi, F., Kim, Y.J. and Chang, B., 2023. A Framework of Deep Optimal Features Selection for Apple Leaf Diseases Recognition. " CMC-COMPUTERS MATERIALS & CONTINUA, 75(2023), pp.697-714.
[21] Al-Khazraji, H., Nasser, A.R., Hasan, A.M., Al Mhdawi, A.K., Al-Raweshidy, H. and Humaidi, A.J., 2022. Aircraft engines remain useful for life prediction based on a hybrid model of autoencoder and deep belief network. IEEE Access, 10, pp.82156-82163.
[22] Du, Y., Yuan, H., Jia, K. and Li, F., 2023. Research on Threshold Segmentation Method of Two-dimensional Otsu Image Based on Improved Sparrow Search Algorithm. IEEE Access.

Doi: https://doi.org/10.54216/FPA.140210
Received: July 17, 2023 Revised: November 09, 2023 Accepted: January 08, 2024